BaBar explores CP violation

Y. Karyotakis

LAPP-EXP 2002-12
December 2002

BaBar explores CP violation

Y. Karyotakis
On behalf of the BaBar Collaboration

LAPP-IN2P3-CNRS
9 chemin de Bellevue - BP. 110
F-74941 Annecy-le-Vieux Cedex

31th International Conference on High Energy Physics
Amsterdam (Netherlands), July 24-31, 2002

BABAR explores CP violation

Y.Karyotakis[a]

[a]SLAC and Laboratoire de Physique de Particules d'Annecy le Vieux
On behalf of the *BABAR* experiment

The most recent results obtained by the *BABAR* experiment at the PEP-II asymmetric-energy B Factory at SLAC on CP-violating asymmetries and branching fractions for neutral and charged B decays are presented here. The analysis was performed on a data sample of ~ 88 million $\Upsilon(4S) \to B\overline{B}$ decays collected between 1999 and 2002. Using $b \to c\bar{c}s$ decays, we measure $\sin 2\beta = 0.741 \pm 0.067$ (stat) ± 0.034 (syst). We also present $\sin 2\beta$ measurements from, $b \to s\bar{s}s$ and $b \to c\bar{c}d$ processes. From neutral B meson decays to two-body final states of charged pions and kaons, we derive for the CP violating parameters, $S_{\pi\pi} = 0.02 \pm 0.34 \pm 0.05$ $[-0.54, +0.58]$ and $C_{\pi\pi} = -0.30 \pm 0.25 \pm 0.04$ $[-0.72, +0.12]$. First results for $B \to \pi^+\pi^-\pi^0$ and $K^\pm\pi^\mp\pi^0$ final states dominated by the $\rho^\pm$ resonance, are also presented.

1. Introduction

The Standard Model of electroweak interactions describes *CP* violation in weak interactions as a consequence of a complex phase in the three-generation Cabibbo-Kobayashi-Maskawa (CKM) quark-mixing matrix[1]. From the CKM unitarity we derive six relationships between its elements, V_{ij}, forming triangles in the complex plane. In this framework, measurements of *CP* asymmetries in the proper-time distribution of neutral B decays to *CP* eigenstates, provide a direct measurement for the angles of the unitarity triangle, $V_{ud}V_{ub}^* + V_{cd}V_{cb}^* + V_{td}V_{tb}^* = 0$. In the most general case the decay rate asymmetry as a function of time, $A_{CP}(\Delta t)$ between a B^0 and a $\overline{B}^0$ can be written as a function of two coefficients S_f and C_f, depending on the final state, f.

$$A_{CP}(\Delta t) = S_f \sin(\Delta m_d \Delta t) - C_f \cos(\Delta m_d \Delta t), \quad (1)$$

where $\Delta t = t_{\rm rec} - t_{\rm tag}$ is the difference between the proper decay times of the reconstructed B meson ($B_{\rm rec}$) and the tagging B meson ($B_{\rm tag}$), Δm_d is the mixing frequency due to the eigenstate mass difference and the parameters S_f and C_f are defined as

$$S_f \equiv \frac{2\,\mathcal{I}m\lambda_f}{1+|\lambda_f|^2} \quad \text{and} \quad C_f \equiv \frac{1-|\lambda_f|^2}{1+|\lambda_f|^2}, \qquad (2)$$

where $\lambda_f = \frac{q}{p}\frac{\bar{A}(f)}{A(f)}$, with $A(f)$ and $\bar{A}(f)$ being the decay amplitudes leading to the final state f.

The sine term in equation 1 is due to the interference between direct decay and decay after flavour change, and when only one amplitude is contributing to the final state, it measures the sine of one of the unitarity triangle angles, α, β or γ. The cosine term is due to the interference between two or more decay amplitudes, a tree and a penguin for example, with different weak and strong phases. In this case the angle involved in the sine term, is modified by a strong phase and doesn't measure directly, α, β or γ. Notice, a cosine term different from zero, is a proof of direct *CP* violation.

New physics, for example a coupling between super-symmetric and Standard Model fields, introduces new phases which may reshape the unitarity triangle. It is therefore very important to check the triangle consistency as precisely as possible, measuring the sides and the angles.

Both *BABAR* [2] and Belle [3] collaborations have established *CP* violation in neutral B decays. These results are consistent with the Standard Model expectations based on measurements and theoretical estimates of the magnitudes of the elements of the Cabibbo-Kobayashi-Maskawa quark-mixing matrix.

2. The *BABAR* experiment

The *BABAR* detector is located at the unique interaction region IR6, of the PEP-II rings at SLAC, running at a center of mass energy almost equal to the $\Upsilon(4S)$ mass. The best peak luminosity achieved by the accelerator is $4.6 \times 10^{33}\,\mathrm{cm}^{-2}\mathrm{s}^{-1}$ for a designed value of $3.0 \times 10^{33}\,\mathrm{cm}^{-2}\mathrm{s}^{-1}$. PEP-II has delivered since October 1999, $99\,\mathrm{fb}^{-1}$. *BABAR* has accumulated $81.2\,\mathrm{fb}^{-1}$ on the $\Upsilon(4S)$ peak and $9.6\,\mathrm{fb}^{-1}$ 40 MeV below, for background subtraction. The overall experiment's efficiency is $\sim 96\%$.

The $\Upsilon(4S)$ resonance decays, with 50% branching fraction to a coherent pair of a B^0 and $\overline{B}^0$ oscillating with exactly the opposite flavor, until one of the B decays. A time dependent asymmetry measurement implies, to fully reconstruct the final state of one B ($B_{\rm rec}$), the flavor tagging of the remaining B meson ($B_{\rm tag}$), and the measurement of the time difference Δt between the two Bs.

A detailed description of the *BABAR* detector is presented in Ref.[4]. Charged particle (track) momenta are measured in a tracking system consisting of a 5-layer double-sided silicon vertex tracker (SVT) and a 40-layer drift chamber (DCH) filled with a gas mixture of helium and isobutane. The SVT and DCH operate within a 1.5 T superconducting solenoidal magnet. The typical decay vertex resolution for reconstructed B decays is approximately $65\,\mu$m along the center-of-mass (CM) boost direction. Photons are detected in an electromagnetic calorimeter (EMC) consisting of 6580 CsI(Tl) crystals arranged in barrel and forward endcap subdetectors. The flux return for the solenoid is composed of multiple layers of iron and resistive plate chambers for the identification of muons and long-lived neutral hadrons.

Particle identification is the key issue for many important analysis, like $B^0 \to \pi^+\pi^-$, $K^+\pi^-$, K^+K^- decays. Tracks are identified as pions or kaons by the Cherenkov angle θ_c measured with a detector of internally reflected Cherenkov light (DIRC). The typical separation between pions and kaons varies from 8σ at $2\,\mathrm{GeV}/c$ to 2.5σ at $4\,\mathrm{GeV}/c$, where σ is the average resolution on θ_c. Lower momentum kaons used in B flavor tagging are identified with a selection algorithm that combines θ_c (for momenta down to $0.6\,\mathrm{GeV}/c$) with measurements of ionization energy loss dE/dx in the DCH and SVT. The selection efficiency is approximately 85% for a pion misidentification probability of 2.5%.

We use a multivariate technique [2] to determine the flavor of the $B_{\rm tag}$ meson. Separate neural networks are trained to identify primary leptons, kaons, soft pions from D^* decays, and high-momentum charged particles from B decays. Events are assigned to one of five mutually exclusive tagging categories based on the estimated mistag probability and the source of the tagging information. The quality of tagging is expressed in terms of the effective efficiency $Q = \sum_k \epsilon_k(1-2w_k)^2$, where ϵ_k and w_k are the efficiencies and mistag probabilities, respectively, for events tagged in category k. The overall tagging efficiency measured in a data sample $B_{\rm flav}$ of fully reconstructed neutral B decays to $D^{(*)-}(\pi^+,\,\rho^+,\,a_1^+)$, is $(28.4 \pm 0.7)\%$.

The time interval Δt between the two B decays is calculated from the measured separation Δz between the decay vertices of $B_{\rm rec}$ and $B_{\rm tag}$ along the collision (z) axis [5]. The r.m.s. Δt resolution is 1.1 ps.

3. $\sin 2\beta$ measurement

A precise measurement of $\sin 2\beta$ can be obtained using the golden decays, $b \to c\bar{c}s$, containing a charmonium meson in the final state. In addition other decays, $b \to d\bar{d}s$ or $b \to s\bar{s}s$, under some conditions also measure $\sin 2\beta$. Looking for differences between all the measured values, may lead to new physics.

3.1. $b \to c\bar{c}s$

This mode is the cleanest, both from the theoretical and experimental point of view. Penguin contributions are suppressed by $\lambda^2_{Cabibbo}$, or have the same weak phase. No direct CP violation is expected in the Standard Model, and the asymmetry can be simply written as:

$$A_{CP}(\Delta t) \equiv -\eta_f \sin 2\beta \sin(\Delta m_d\,\Delta t) \qquad (3)$$

with $\eta_f = -1$ for $J/\psi\,K^0_S$, $\psi(2S)K^0_S$, $\chi_{c1}K^0_S$, and $\eta_c K^0_S$, and $+1$ for $J/\psi\,K^0_L$. Due to the presence

of even (L=0, 2) and odd (L=1) orbital angular momenta in the $B \to J/\psi K^{*0}$ final state, there can be CP-even and CP-odd contributions to the decay rate. When the angular information in the decay is ignored, the measured CP asymmetry in $J/\psi K^{*0}$ is reduced by a factor $1-2R_\perp$, where $R_\perp$ is the fraction of the L=1 component. We have measured $R_\perp = (16.0 \pm 3.5)\%$ [7], which gives $\eta_f = 0.65 \pm 0.07$ after acceptance corrections in the $J/\psi K^{*0}$ mode.

Experimentally the involved branching fractions are rather high, and the final state reconstruction, with a K^0_S benefits from little background, as shown in figure 1.

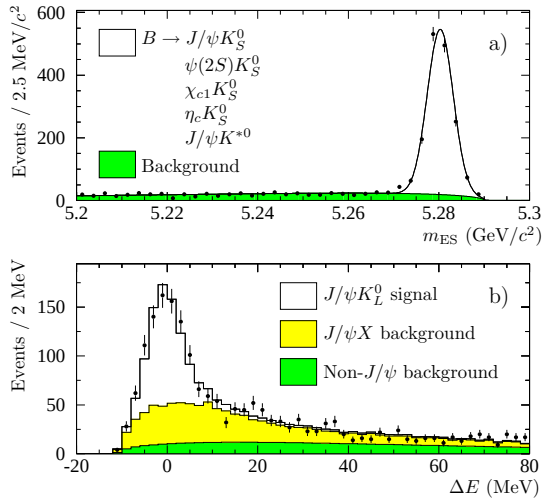

Figure 1. Distributions for B_{CP} candidates satisfying the tagging and vertexing requirements: a) $m_{\rm ES}$ for the final states $J/\psi K^0_S$, $\psi(2S)K^0_S$, $\chi_{c1}K^0_S$, $\eta_c K^0_S$, and $J/\psi K^{*0}(K^{*0} \to K^0_S\pi^0)$, b) ΔE for the final state $J/\psi K^0_L$.

We observe 2641 events after tagging and vertexing. Table 1 summarizes the number of events per channel, the signal purity, and the fitted sin2β value. Figure 2 shows the Δt distributions and asymmetries in yields between B^0 tags and $\overline{B}^0$ tags for the $\eta_f = -1$ sample as a function of Δt, overlaid with the projection of the likelihood fit result.

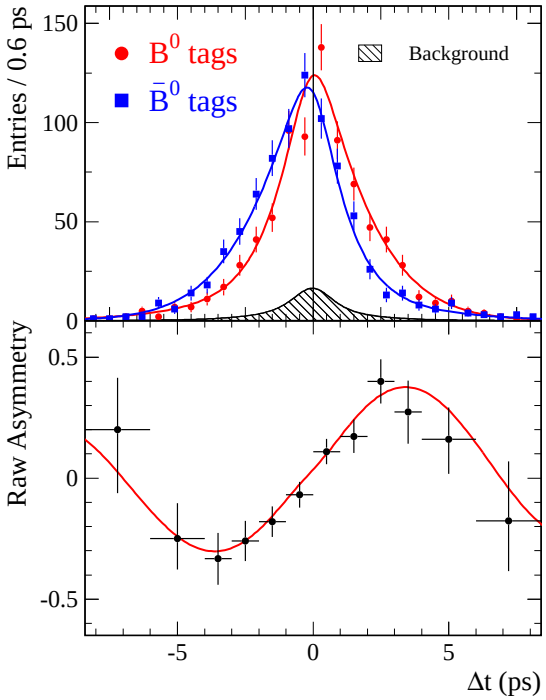

Figure 2. Top) Number of $\eta_f = -1$ candidates ($J/\psi K^0_S$, $\psi(2S)K^0_S$, $\chi_{c1}K^0_S$, and $\eta_c K^0_S$) in the signal region with a B^0 tag and with a $\overline{B}^0$ tag and bottom) the raw asymmetry $(N_{B^0}-N_{\overline{B}^0})/(N_{B^0}+N_{\overline{B}^0})$ as functions of Δt. The red (blue) curves represent the fit projection in Δt for B^0 ($\overline{B}^0$) tags. The shaded regions represent the background contributions.

From a simultaneous unbinned maximum likelihood fit to the Δt distributions of the tagged B_{CP} and $B_{\rm flav}$ samples, taking into account the Δt resolution, the tagging efficiency and the mistag rate, we measure [6] :

$$\sin2\beta = 0.741 \pm 0.067\ (\text{stat}) \pm 0.034\ (\text{syst})$$

This new value, improves both the statistical and systematic error, and it is consistent with our previous published results [2]. It is also consistent with the range implied by indirect measurements and theoretical estimates, as shown in figure 3.

From a fit only to the $\eta_f = -1$ sample, allowing for a non zero coefficient C_f of equation 1, we measure $|\lambda_{c\bar{c}s}| = 0.948 \pm 0.051$ (stat) $\pm$ 0.030 (syst), consistent with one, as expected from the Standard Model. In this case the coefficient of the $\sin(\Delta m_d \Delta t)$ term in Eq. 1 is measured to be 0.759 ± 0.074 (stat).

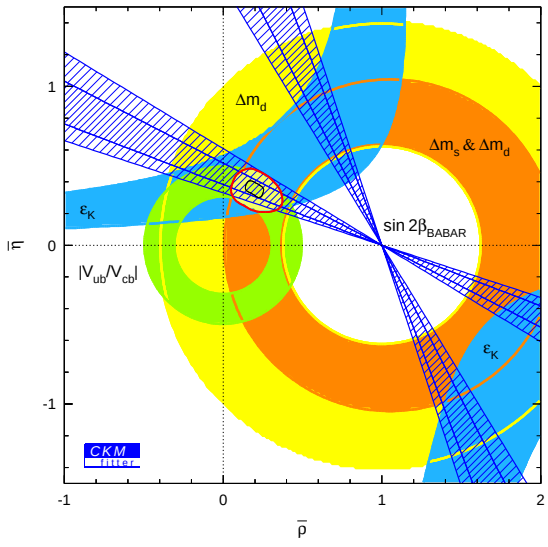

Figure 3. The red contour shows the allowed region for the unitarity triangle apex, as obtained from indirect measurements and theoretical calculations. In blue, the one and two sigma contours from the sin2β measurement [8].

3.2. CP asymmetries in the decay $B^0 \to D^{*+}D^{*-}$

The $B^0 \to D^{*+}D^{*-}$ decay is a Cabibbo suppressed transition, $b \to c\bar{c}d$, dominated by the tree diagram. The CP asymmetry measures sin2β ($\beta \equiv \arg\left[-V_{\rm cd}V_{\rm cb}^*/V_{\rm td}V_{\rm tb}^*\right]$) to be compared with -sin2β from $b \to c\bar{c}s$. However a small penguin contribution is also expected [9]. In addition $B^0 \to D^{*+}D^{*-}$ is a pseudoscalar decay to a vector-vector final state, which requires the measurement of the *CP*-odd fraction, $R_\perp$.

$$R_\perp = \frac{M_\perp^2}{M_0^2 + M_\parallel^2 + M_\perp^2} \qquad (4)$$

where M_i are the decay amplitudes for the three partial waves, L=0,1,2. The angular distribution of the decay products expressed as a function of the transversity angle θ_{tr}, is given by:

$$\frac{1}{\Gamma}\frac{{\rm d}\Gamma}{{\rm d}\cos\theta_{\rm tr}} = \frac{3}{4}(1-R_\perp)\sin^2\theta_{\rm tr} + \frac{3}{2}R_\perp\cos^2\theta_{\rm tr} \qquad (5)$$

From un unbinned maximum likelihood fit of $\cos\theta_{\rm tr}$ to our data, we measure [10] :

$$R_\perp = 0.07 \pm 0.06(stat) \pm 0.03(syst).$$

A priori sizeable penguin contribution can not be excluded, and therefore the weak phase difference $\mathrm{Im}(\lambda_{D^{*+}D^{*-}}) = -\sin 2\beta$ can be affected. The value of $\lambda_{D^{*+}D^{*-}}$ can be different for the three transversity amplitudes because of possible different penguin-to-tree ratios. We include all these contributions in the parametrization of the decay rates which are now given by:

$$f_\pm(\Delta t) = \frac{{\rm e}^{-|\Delta t|/\tau_{B^0}}}{4\tau_{B^0}}\Big\{O(1 - \tfrac{1}{2}\Delta\mathcal{D}) \mp \mathcal{D}\left[S\sin\left(\Delta m_d\Delta t\right) + C\cos\left(\Delta m_d\Delta t\right)\right]\Big\} \qquad (6)$$

where $\mathcal{D}$, is the dilution factor due to the mistags and the coefficients O, C and S depend on λ_+ and $\lambda_\perp$ parameters related to the *CP*-odd and *CP*-even states.

This analysis benefits from our high efficiency on low momentum track reconstruction. From 126 ± 13 $D^{*+}D^{*-}$ that we observe, we fit $|\lambda_+|$ and $\mathrm{Im}(\lambda_+)$. As the *CP*-odd fraction is small we fix $|\lambda_\perp| = 1$ and $\mathrm{Im}(\lambda_\perp) = -0.741$. The results [10] obtained from the fit (Fig. 4) are as follows:

$$\begin{aligned} \mathrm{Im}(\lambda_+) &= 0.31 \pm 0.43(stat) \pm 0.13(syst) \\ |\lambda_+| &= 0.98 \pm 0.25(stat) \pm 0.09(syst). \end{aligned}$$

Sample	$N_{\rm tag}$	$P(\%)$	sin2β
$J/\psi K^0_S$,$\psi(2S)K^0_S$,$\chi_{c1}K^0_S$,$\eta_c K^0_S$	1506	94	0.76 ± 0.07
$J/\psi K^0_L$ ($\eta_f = +1$)	988	55	0.72 ± 0.16
$J/\psi K^{*0}(K^{*0} \to K^0_S\pi^0)$	147	81	0.22 ± 0.52
Full *CP* sample	2641	78	0.74 ± 0.07
$J/\psi K^0_S$, $\psi(2S)K^0_S$, $\chi_{c1}K^0_S$, $\eta_c K^0_S$ only ($\eta_f = -1$)			
$J/\psi K^0_S$ ($K^0_S \to \pi^+\pi^-$)	974	97	0.82 ± 0.08
$J/\psi K^0_S$ ($K^0_S \to \pi^0\pi^0$)	170	89	0.39 ± 0.24
$\psi(2S)K^0_S$ ($K^0_S \to \pi^+\pi^-$)	150	97	0.69 ± 0.24
$\chi_{c1}K^0_S$	80	95	1.01 ± 0.40
$\eta_c K^0_S$	132	73	0.59 ± 0.32
B^0 tags	740	94	0.76 ± 0.10
$\overline{B}^0$ tags	766	93	0.75 ± 0.10
$B_{\rm flav}$ sample	25375	85	0.02 ± 0.02
B^+ sample	22160	89	0.02 ± 0.02

Table 1
Number of events $N_{\rm tag}$ in the signal region after tagging and vertexing requirements, signal purity P, and results of fitting for *CP* asymmetries in the B_{CP} sample and in various subsamples, as well as in the $B_{\rm flav}$ and charged B control samples. Errors are statistical only.

Im(λ_+) has to be compared with $-\sin 2\beta = -0.741 \pm 0.067$ from the golden modes. More data are needed to establish contributions from penguin diagrams or a difference with the $b \to c\bar{c}s$ process.

3.3. CP asymmetries in the decay $B^0 \to J/\psi\pi^0$

$B^0 \to J/\psi\pi^0$ is an other Cabibbo suppressed, $b \to c\bar{c}d$ decay. The tree contribution has the same weak phase as the $b \to c\bar{c}s$ and measures -sin2β. However in this case large penguin contributions are expected. Both tree and penguin diagrams contribute proportional to $\lambda^3_{Cabibbo}$. The weak phase of a portion of the penguin is different from the tree and both $S_{J/\psi\pi^0}$ and $C_{J/\psi\pi^0}$ should be non zero.

We measure [11] $S_{J/\psi\pi^0}$ and $C_{J/\psi\pi^0}$ by an unbinned maximum likelihood fit to 438 events consisting of signal events, $B^0 \to J/\psi K^0_S(\pi^0\pi^0)$, inclusive J/ψ, $B\overline{B}$, and continuum background. Figure 5 shows the beam constrained mass, $m_{\rm ES}$, distribution for the signal and all four backgrounds. 40 ± 7 signal events are observed. The coefficients of the sinus and cosinus terms of the time dependent asymmetry in equation 1, are then measured as:

$$S_{J/\psi\pi^0} = 0.05 \pm 0.49(stat) \pm 0.16(syst)$$
$$C_{J/\psi\pi^0} = 0.38 \pm 0.41(stat) \pm 0.09(syst)$$

Given the large statistical errors, there is no evidence for direct *CP* violation, and the comparison of $S_{J/\psi\pi^0}$ with the golden channels doesn't bring new information. With increasing statistics in the future this channel will become quiet interesting as it also probes penguin contributions usually neglected in the golden modes.

3.4. sin2β from $B^0 \to \phi K^0_S$

The charmless hadronic decay, $B^0 \to \phi K^0_S$, is dominated by the $b \to s\bar{s}s$ gluonic penguins, figure 6. All other Standard model contributions are highly suppressed. The *CP* asymmetry measures sin2β, and only a 4% deviation is expected from the golden modes. The presence of the penguin loops, and the possibility to reveal new physics, make this channel very interesting. *BABAR* has measured with 45M $B\overline{B}$ pairs a branching ratio of $BF(B^0 \to \phi K^0) = (8.1^{+3.1}_{-2.5} \pm 0.8) \times 10^{-6}$ [12].

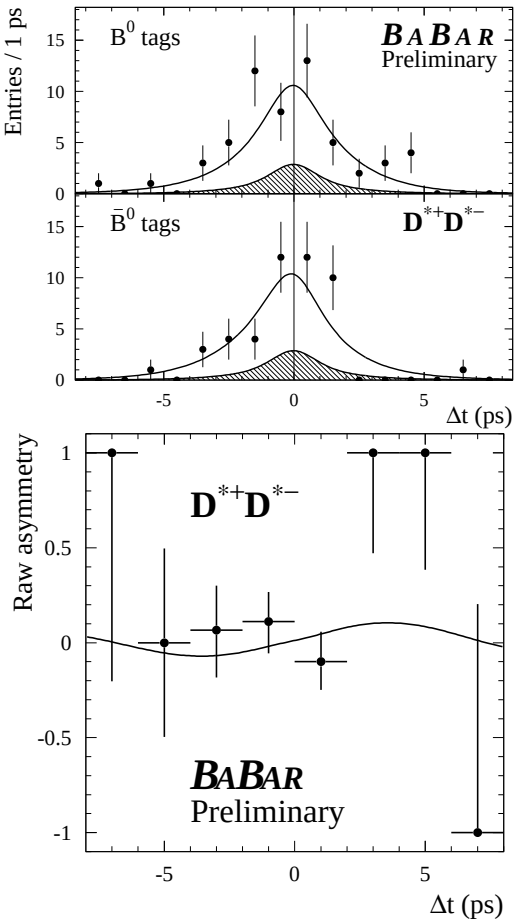

Figure 4. From top to bottom: number N_{B^0} of candidate events in the signal region ($B^0 \to D^{*+}D^{*-}$) with a B^0 tag, number $N_{\overline{B}^0}$ of candidates with a $\overline{B}^0$ tag, and the raw asymmetry $(N_{B^0} - N_{\overline{B}^0})/(N_{B^0} + N_{\overline{B}^0})$, as functions of Δt. The solid curves represent the result of the combined fit to the full sample. The shaded regions represent the background contributions.

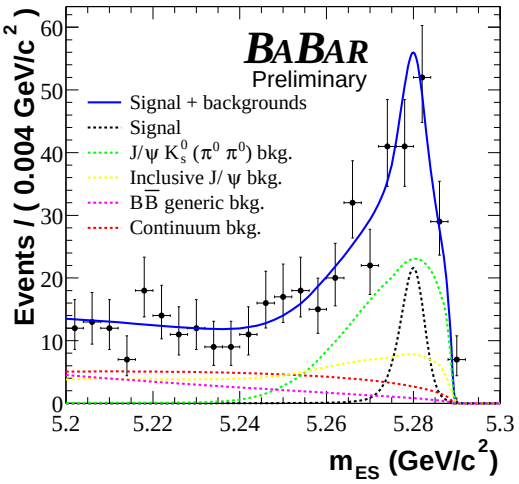

Figure 5. $m_{\rm ES}$, distribution for the signal $B^0 \to J/\psi\pi^0$ and all backgrounds

B mesons candidates are reconstructed in the decay mode $B^0 \to \phi K^0_S$ with $K^0_S \to \pi^+\pi^-$ and $\phi \to K^+K^-$. Figure 7 shows the $m_{\rm ES}$ distribution after tight cuts to reject a large background fraction. From a simultaneous unbinned maximum likelihood fit we find 51 signal, and 1301 background events. From the Δt distribution for B^0 and $\overline{B}^0$ events, fixing $|\lambda_{\phi K^0_S}| = 1$, we extract sin2$\beta$ [13]:

$$\sin 2\beta = -0.19^{+0.52}_{-0.50}(stat) \pm 0.09(syst)$$

This result, dominated by the statistical error, differs of about two standard deviations from sin2β from the golden modes. However also in this case much more luminosity is needed before draw any conclusions.

4. sin2α measurement

Measuring sin2α is considerably more difficult than sin2β from the golden modes. There is no a single decay channel where only a tree diagramme contributes. On the contrary, in all the cases, important penguin contributions, pollute the weak phase difference 2α by an extra contribution, κ. Experimentalists do not measure α but α effective, α_{eff}, with $2\alpha_{eff} = 2\alpha + \kappa$. Depending on the decay channel and using other measurements or theoretical predictions, one could in principle,

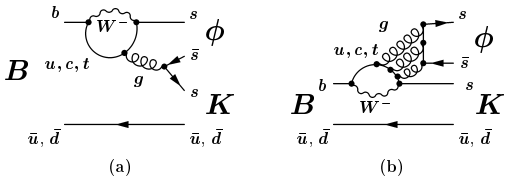

Figure 6. Quark-level diagrams describing the decays $B \to \phi K$: (a) internal penguin, (b) flavor-singlet penguin.

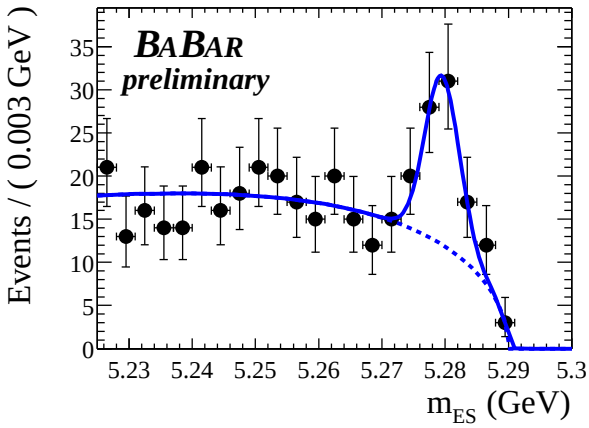

Figure 7. $m_{\rm ES}$ distribution for $B^0 \to \phi K^0_S$ after tight signal selection criteria.

extract α. On the experimental side, the situation is also difficult. The involved branching ratios are small, $\sim 10^{-6}$, and the background quite high. Measuring even α_{eff} is quite challenging.

4.1. *CP* asymmetries in the decay $B^0 \to \pi^+\pi^-$

For this decay mode the tree's diagramme weak phase is $\beta+\gamma$, while the penguin diagramme contributes with both a weak phase $-\beta$ and a strong phase δ. In this case $S_{\pi\pi} = \sqrt{1-C_{\pi\pi}}sin\alpha_{eff}$ with $C_{\pi\pi} \sim sin(\delta)$. Therefore $C_{\pi\pi}$ is expected to be different from zero, and direct *CP* violation should show up.

The key issue for this analysis is particle identification at high momentum. Using the DIRC and dE/dx information, from a control sample of $D^{*+} \to D^0\pi^+$, $D^0 \to K^-\pi^+$ decays, reconstructed from our data, we measure a typical separation between pions and kaons variyng from $8\sigma_{\theta_c}$ at $2\,{\rm GeV}/c$ to $2.5\sigma_{\theta_c}$ at $4\,{\rm GeV}/c$, where θ_c is the Cherenkov angle. For an efficiency of 85% the probability of a kaon to be identified as a pion is 1.7% while the probability for a pion to be identified as a kaon is 2.7%.

Background events from the continuum $e^+e^- \to q\bar{q}$ $(q = u, d, s, c)$ are rejected using a number of topological variables [14].

We build probability density functions (PDF) for signal and background relevant variables and we perform an unbinned maximum likelihood fit, ignoring tagging and Δt information, to extract the branching fractions and the direct *CP* asymmetry, $A_{K\pi} = \frac{B^0\to K^+\pi^- - B^0\to K^-\pi^+}{B^0\to K^+\pi^- + B^0\to K^-\pi^+}$. Table 2 summarizes the signal efficiencies, the branching ratios and the direct *CP* asymmetry (only $B^0 \to K^+\pi^-$) measurements for $B^0 \to \pi^+\pi^-, K^+\pi^-, K^+K^-$.

To validate our fit procedure and the data quality we measure Δm_d and the B^0 life time τ using the sample $B^0 \to K\pi$. We find $\Delta m_d = (0.52 \pm 0.05)\,{\rm ps}^{-1}$ and $\tau = (1.56 \pm 0.07)\,{\rm ps}$, in very good agreement with the world averages.

To determine $S_{\pi\pi}$ and $C_{\pi\pi}$ we include tagging and Δt information in the unbinned maximum likelihood. The Δt PDF for signal $K^+\pi^-$ events takes into account B^0–$\overline{B}^0$ mixing based on the charge of the kaon and the flavor of $B_{\rm tag}$. From

Table 2
Summary of results for total detection efficiencies, fitted signal yields N_S, charge-averaged branching fractions $\mathcal{B}$, and $\mathcal{A}_{K\pi}$. Branching fractions are calculated assuming equal rates for $\Upsilon(4S) \to B^0\overline{B}^0$ and B^+B^-. The upper limits for $N_{K^+K^-}$ and $\mathcal{B}(B^0 \to K^+K^-)$ correspond to the 90% C.L.

Mode	Efficiency (%)	N_S	$\mathcal{B}(10^{-6})$	$\mathcal{A}_{K\pi}$	$\mathcal{A}_{K\pi}$ 90% C.L.
$\pi^+\pi^-$	38.0 ± 0.8	$157 \pm 19 \pm 7$	$4.6 \pm 0.6 \pm 0.2$		
$K^+\pi^-$	37.5 ± 0.8	$589 \pm 30 \pm 17$	$17.9 \pm 0.9 \pm 0.7$	$-0.102 \pm 0.050 \pm 0.016$	$[-0.188, -0.016]$
K^+K^-	36.2 ± 0.8	$1 \pm 8\,(< 16)$	< 0.6		

this fit we find :

$$S_{\pi\pi} = 0.02 \pm 0.34\,(\text{stat}) \pm 0.05\,(\text{syst})$$
$$[-0.54, +0.58]$$
$$C_{\pi\pi} = -0.30 \pm 0.25\,(\text{stat}) \pm 0.04\,(\text{syst})$$
$$[-0.72, +0.12]$$

where the range in square brackets indicates the 90% C.L. interval taking into account the systematic errors. Figure 9 shows the Δt distribution for B^0 and $\overline{B}^0$ events and the asymmetry, $A_{\pi\pi}(\Delta t)$. There is no evidence for direct CP violation within the present errors.

From α_{eff} to α

In order to extract α or the extra angle pollution κ, from $B^0 \to \pi^+\pi^-$ in the most general case a full isospin analysis is required [15]. One has to measure the branching fractions $\mathcal{B}(B^\pm \to \pi^\pm\pi^0)$, $\mathcal{B}(B^0 \to \pi^+\pi^-)$, and $\mathcal{B}(B \to \pi^0\pi^0)$ for both B^0 and $\overline{B}^0$. If $\mathcal{B}(B \to \pi^0\pi^0)$ is small then using only an averaged measurement of $\mathcal{B}(B \to \pi^0\pi^0) = \frac{1}{2}(\mathcal{B}(B^0 \to \pi^0\pi^0) + \mathcal{B}(\overline{B}^0 \to \pi^0\pi^0))$, an upper bound[16] on κ can be derived :

$$|2\alpha - 2\alpha_{eff}| \leq \arccos\frac{1}{\sqrt{1 - C_{\pi\pi}^2}} \times \left(1 - 2\frac{\mathcal{B}(B \to \pi^0\pi^0)}{\mathcal{B}^\pm \to \pi^\pm\pi^0}\right) \quad (7)$$

We have measured [17] the branching fractions for $B^+ \to \pi^+\pi^0$, $B^+ \to K^+\pi^0$ and $B^0 \to K^0\pi^0$ decays as well as the direct CP asymmetries integrated over the time. For the $K^0\pi^0$ mode we need to measure the flavor of the B candidate in order to extract the CP asymmetry.

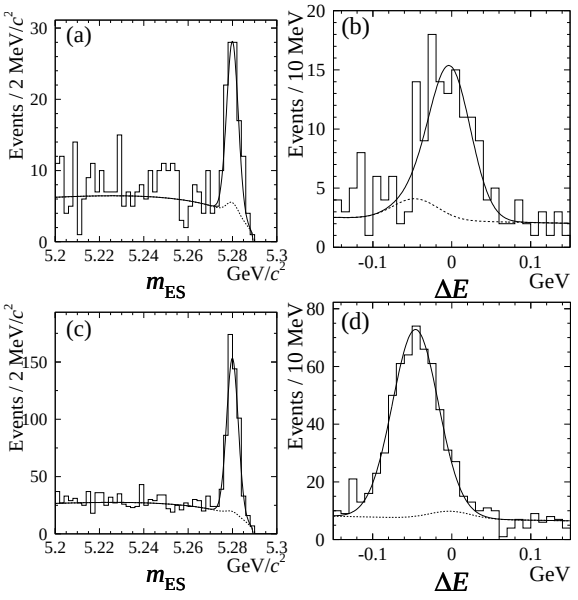

Figure 8. Distributions of $m_{\rm ES}$ and ΔE for events enhanced in signal (a), (b) $\pi^+\pi^-$ and (c), (d) $K^\mp\pi^\pm$ decays. Solid curves represent projections of the maximum likelihood fit, dashed curves represent $q\bar{q}$ and $\pi\pi \leftrightarrow K\pi$ cross-feed background.

Table 3
Summary of fitted signal yields, measured branching fraction $\mathcal{B}$ and *CP* asymmetries $\mathcal{A}_i$. The first error is statistical and the second is systematic.

Mode	Signal Yield	$\mathcal{B}\,(10^{-6})$	$\mathcal{A}_i$	$\mathcal{A}_i$ (90% CL)
$\pi^+\pi^0$	$125^{+23}_{-21} \pm 10$	$5.5^{+1.0}_{-0.9} \pm 0.6$	$-0.03^{+0.18}_{-0.17} \pm 0.02$	$[-0.32, 0.27]$
$K^+\pi^0$	$239^{+21}_{-22} \pm 6$	$12.8^{+1.2}_{-1.1} \pm 1.0$	$-0.09 \pm 0.09 \pm 0.01$	$[-0.24, 0.06]$
$K^0\pi^0$	$86 \pm 13 \pm 3$	$10.4 \pm 1.5 \pm 0.8$	$0.03 \pm 0.36 \pm 0.09$	$[-0.58, 0.64]$

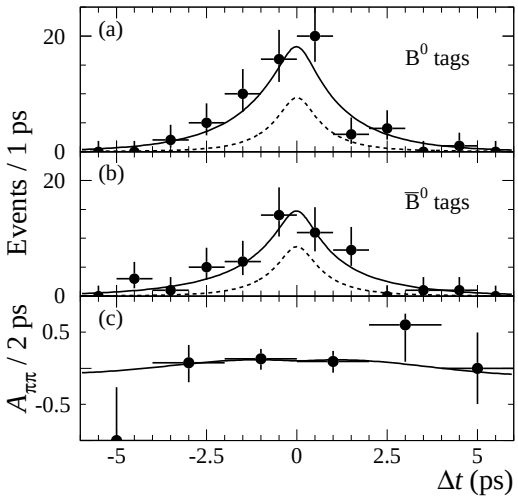

Figure 9. Distributions of Δt for events enhanced in signal $\pi\pi$ decays with $B_{\rm rec}$ tagged as (a) B^0 or (b) $\overline{B}^0$, and (c) the asymmetry $\mathcal{A}_{\pi\pi}(\Delta t)$ as a function of Δt. Solid curves represent projections of the maximum likelihood fit, dashed curves represent the sum of $q\bar{q}$ and $K\pi$ background events.

Clear signals are observed for all three decay modes, and the direct *CP* asymmetry is measured. All the results are summarized on Table 3. No direct *CP* violation is observed.

The analysis of $B \to \pi^0\pi^0$ is very challenging. The expected branching ratio is small, and we have to fight against an important background from $q\bar{q}$ events and $B^\pm \to \rho^\pm\pi^0$ decays. In addition to topological variables, we use the tagging information to further reduce the background. Our overall efficiency is 16.5%. After un unbinned maximum likelihood fit, we observe 23^{+10}_{-9} events. We then extract an upper limit for the branching fraction of $B \to \pi^0\pi^0$ [18]:

$$\mathcal{B}(B \to \pi^0\pi^0) < 3.6 \times 10^{-6}$$
at 90% confidence level

The rather high value of this limit, gives a loose bound for $|2\alpha - 2\alpha_{eff}| < 51°$, Figure 10. If the branching ratio is higher than 1.5 or 2×10^{-6}, we will have to perform the complete isospin analysis, as the Grossman-Quin bound will not constrain α enough.

4.2. *CP* asymmetries in the decays $B \to \pi^+\pi^-\pi^0$ and $B \to K^\pm\pi^\mp\pi^0$ final states

For these modes we restrict the analysis to the only final states dominated by the $\rho^\pm$ resonance. As in the case of $B \to \pi^+\pi^-$, the $\rho\pi$ mode also measures α as well as direct *CP* violation. However it is not a *CP* eigenstate and four amplitudes have to be considered, $\overline{B}^0 \to \pi^-\rho^+$, $B^0 \to \pi^-\rho^+$, $B^0 \to \pi^+\rho^-$ and $\overline{B}^0 \to \pi^+\rho^-$. The decay rate distributions can be written as [19] :

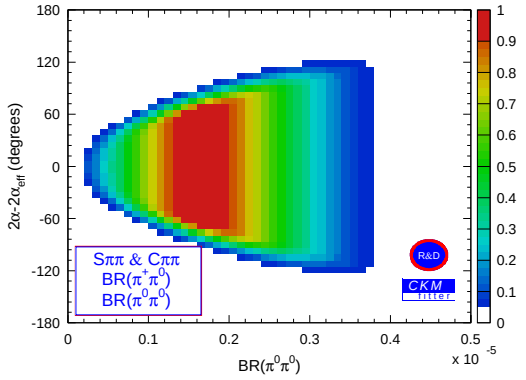

Figure 10. $B \to \pi^0\pi^0$ branching fraction versus $2\alpha - 2\alpha_{eff}$

$$f^{\rho^\pm h^\mp}_{B^0\text{tag}}(\Delta t) = (1 \pm A^{\rho h}_{CP})\frac{e^{-|\Delta t|/\tau}}{4\tau} \times \left[1 + \Big((S_{\rho h} \pm \Delta S_{\rho h})\sin(\Delta m_d \Delta t) - (C_{\rho h} \pm \Delta C_{\rho h})\cos(\Delta m_d \Delta t)\Big)\right],$$
$$f^{\rho^\pm h^\mp}_{\overline{B}^0\text{tag}}(\Delta t) = (1 \pm A^{\rho h}_{CP})\frac{e^{-|\Delta t|/\tau}}{4\tau} \times \left[1 - \Big((S_{\rho h} \pm \Delta S_{\rho h})\sin(\Delta m_d \Delta t) - (C_{\rho h} \pm \Delta C_{\rho h})\cos(\Delta m_d \Delta t)\Big)\right] \quad (8)$$

The time-integrated charge asymmetries $A^{\rho\pi}_{CP}$ and $A^{\rho K}_{CP}$ measure direct CP violation. The time dependence is described by four parameters, $S_{\rho h}$, $C_{\rho h}$, $\Delta C_{\rho h}$ and $\Delta S_{\rho h}$. In the case of the self-tagging ρK mode, the values of these four parameters are known to be $C_{\rho K} = 0$, $\Delta C_{\rho K} = -1$, $S_{\rho K} = 0$, and $\Delta S_{\rho K} = 0$. For the $\rho\pi$ mode, they allow us to probe CP violation. Summing over the ρ charge in Eq. 8, and neglecting the charge asymmetry $A^{\rho\pi}_{CP}$, one obtains the simplified CP asymmetry between the number of B^0 and $\overline{B}^0$ tags, given by:

$$A_{B^0/\overline{B}^0} \sim S_{\rho\pi}\sin(\Delta m_d \Delta t) - C_{\rho\pi}\cos(\Delta m_d \Delta t) \quad (9)$$

The parameter $C_{\rho\pi}$ describes the time-dependent direct CP violation and $S_{\rho\pi}$ measures CP violation in the interference between mixing and decay related to the angle α.

The parameters $\Delta C_{\rho\pi}$ and $\Delta S_{\rho\pi}$ are insensitive to CP violation. The asymmetry between $N(B^0_{\rho\pi} \to \rho^+\pi^-) + N(\overline{B}^0_{\rho\pi} \to \rho^-\pi^+)$ and $N(B^0_{\rho\pi} \to \rho^-\pi^+) + N(\overline{B}^0_{\rho\pi} \to \rho^+\pi^-)$ is described by $\Delta C_{\rho\pi}$, while $\Delta S_{\rho\pi}$ is sensitive to the strong phase difference between the amplitudes contributing to $B^0 \to \rho\pi$ decays. The naive factorization model [20] predicts $\Delta C_{\rho\pi} \sim 0.4$ while there is no prediction for $\Delta S_{\rho\pi}$.

To reduce the main background for these modes, coming from continuum $q\bar{q}$ (where $q = u, d, s, c$) events we use a neural network, combining two kinematic variables and two event shape variables. More than 80 charmless decay modes have been considered for potential cross-feed in the signal region. Fitting simultaneously the signal and background events we find 413^{+34}_{-33} (stat) $\rho\pi$ and 147^{+22}_{-21} (stat) ρK events in our data sample. Figure 11 shows the distributions of $m_{\rm ES}$ and ΔE for data samples that are enhanced in signal using cuts on the signal-to-continuum likelihood ratio of the other discriminating variables. For the CP parameters we then measure [21]:

$$\begin{aligned} A^{\rho K}_{CP} &= 0.19 \pm 0.14\ (\text{stat}) \pm 0.11\ (\text{syst}),\\ A^{\rho\pi}_{CP} &= -0.22 \pm 0.08\ (\text{stat}) \pm 0.07\ (\text{syst}),\\ C_{\rho\pi} &= 0.45\ ^{+0.18}_{-0.19}\ (\text{stat}) \pm 0.09\ (\text{syst}),\\ S_{\rho\pi} &= 0.16 \pm 0.25\ (\text{stat}) \pm 0.07\ (\text{syst}) \end{aligned}$$

The two other observables in the decay rates (Eq. 8) are measured to be

$$\begin{aligned} \Delta C_{\rho\pi} &= 0.38^{+0.19}_{-0.20}\ (\text{stat}),\\ \Delta S_{\rho\pi} &= 0.15 \pm 0.26\ (\text{stat}) \end{aligned}$$

Alternatively, the results on direct CP violation can be expressed using the asymmetries

$$\begin{aligned} A_{+-} &= \frac{N(\overline{B}^0_{\rho\pi} \to \rho^+\pi^-) - N(B^0_{\rho\pi} \to \rho^-\pi^+)}{N(\overline{B}^0_{\rho\pi} \to \rho^+\pi^-) + N(B^0_{\rho\pi} \to \rho^-\pi^+)}\\ &= \frac{A^{\rho\pi}_{CP} - C_{\rho\pi} - A^{\rho\pi}_{CP}\cdot\Delta C_{\rho\pi}}{1 - \Delta C_{\rho\pi} - A^{\rho\pi}_{CP}\cdot C_{\rho\pi}}\,, \end{aligned} \quad (10)$$

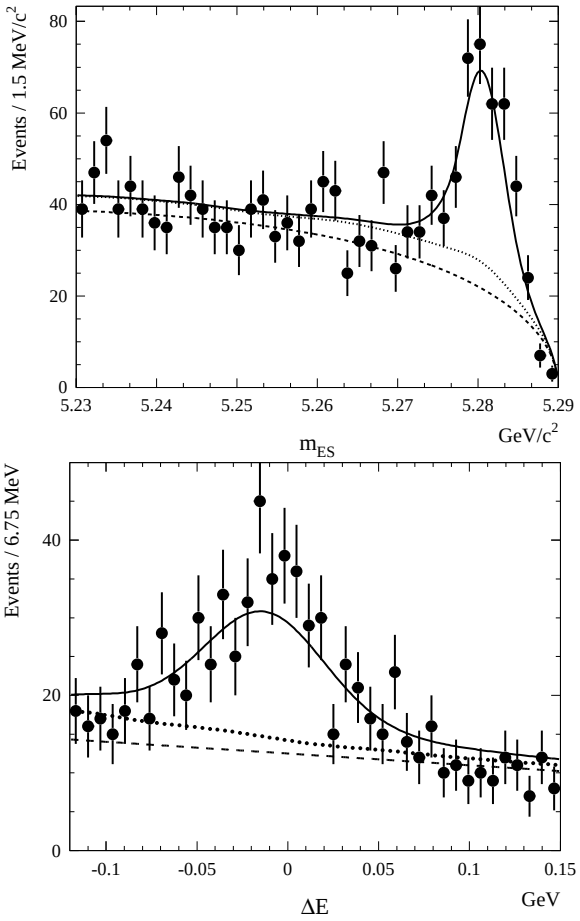

Figure 11. Distributions of $m_{\rm ES}$ and ΔE for samples enhanced in $\rho\pi$ signal using cuts on likelihood ratios. The solid curve represents a projection of the maximum likelihood fit result. The dashed curve represents the contribution from continuum events ($\rho\pi$ and ρK candidates combined), and the dotted line indicates the combined contributions from continuum events and B-related backgrounds, including ρK.

$$A_{-+} = \frac{N(\overline{B}^0_{\rho\pi} \to \rho^-\pi^+) - N(B^0_{\rho\pi} \to \rho^+\pi^-)}{N(\overline{B}^0_{\rho\pi} \to \rho^-\pi^+) + N(B^0_{\rho\pi} \to \rho^+\pi^-)} = -\frac{A^{\rho\pi}_{CP} + C_{\rho\pi} + A^{\rho\pi}_{CP} \cdot \Delta C_{\rho\pi}}{1 + \Delta C_{\rho\pi} + A^{\rho\pi}_{CP} \cdot C_{\rho\pi}} \,. \quad (11)$$

In the decays $\overline{B}^0_{\rho\pi} \to \rho^+\pi^-$ and $B^0_{\rho\pi} \to \rho^-\pi^+$ the spectator quark is involved in the formation of the ρ meson. These two decay modes are related to the direct CP asymmetry A_{+-} according to Eq. 10. Similarly in Eq. 11, we probe direct CP violation through the asymmetry A_{-+} using the decays $\overline{B}^0_{\rho\pi} \to \rho^-\pi^+$ and $B^0_{\rho\pi} \to \rho^+\pi^-$. In this case the π meson is formed from the spectator quark. From the above fitted values we obtain

$$\begin{aligned} A_{+-} &= -0.82 \pm 0.31 \ \text{(stat)} \\ A_{-+} &= -0.11 \pm 0.16 \ \text{(stat)}. \end{aligned} \quad (12)$$

Extracting α from these measurements is not straight forward, and considerable theoretical input is needed.

5. The angle γ

The *BABAR* experiment takes data only on the $\Upsilon(4S)$ resonance, below the B_s threshold, whose decays can be used to measure the angle γ. However it has been proposed [22,23] to use the branching ratios of the processes $B^- \to D^0_{(CP)}K^-$ and $B^\pm \to D^0_{CP}K^\pm$, where D^0_{CP} indicates the CP-even or CP-odd states ($D^0 \pm \overline{D}^0)/\sqrt{2}$ and extract 2γ. As a first step for this analysis we have measured [24] the ratios,

$$R \equiv \frac{\mathcal{B}(B^- \to D^0 K^-)}{\mathcal{B}(B^- \to D^0\pi^-)}$$

and

$$R_{CP} \equiv \frac{\mathcal{B}(B^- \to D^0_{CP}K^-) + \mathcal{B}(B^+ \to D^0_{CP}K^+)}{\mathcal{B}(B^- \to D^0_{CP}\pi^-) + \mathcal{B}(B^+ \to D^0_{CP}\pi^+)}$$

as well as the direct CP asymmetry

$$A_{CP} \equiv \frac{\mathcal{B}(B^- \to D^0_{CP}\,K^-) - \mathcal{B}(B^+ \to D^0_{CP}\,K^+)}{\mathcal{B}(B^- \to D^0_{CP}\,K^-) + \mathcal{B}(B^+ \to D^0_{CP}\,K^+)}$$

We reconstruct three D^0 decay modes, $D^0 \to K^-\pi^+$, $D^0 \to K^-\pi^+\pi^+\pi^-$, $D^0 \to K^-\pi^+\pi^0$ and

we combine them with a kaon or pion to reconstruct the decay $B^- \to D^0_{(CP)}K^-$. We then measure the ratio R for each D^0 mode, and the combined result is :

$R = (8.31 \pm 0.35 \pm 0.20)\%$

From the decay $D^0 \to K^-K^+$ combining with a charged kaon we compute

$R_{CP} = (7.4 \pm 1.7 \pm 0.6)\%$

Then the direct *CP* asymmetry, integrated over time is measured to be :

$A_{CP} = 0.17 \pm 0.23\,^{+0.09}_{-0.07}$

6. Summary

With more than 88M $B\overline{B}$ pairs the *BABAR* experiment has measured a new value for $\sin 2\beta = 0.741 \pm 0.067\,(\text{stat}) \pm 0.034\,(\text{syst})$ extracted from $b \to c\bar{c}s$ decays. Less precise measurements from other modes have also been performed and will allow in the future to probe for new physics effects. We have also measured $S_{\pi\pi} = 0.02 \pm 0.34\,(\text{stat}) \pm 0.05\,(\text{syst})$ and $C_{\pi\pi} = -0.30 \pm 0.25\,(\text{stat}) \pm 0.04\,(\text{syst})$ and start building the full isospin analysis to extract α. We have also studied for the first time the decay $B \to \pi^+\pi^-\pi^0$ dominated by the ρ final states, and measure the *CP* violating parameters. We do not have a strong evidence for direct *CP* violation yet. We expect in the next years, as the integrated luminosity will increase significantly, to bring some answers to the whole picture of the *CP* violation phenomenon.

7. Acknowledgments

We are grateful for the excellent luminosity and machine conditions provided by our PEP-II colleagues, and for the substantial dedicated effort from the computing organizations that support *BABAR*. The collaborating institutions wish to thank SLAC for its support and kind hospitality. This work is supported by DOE and NSF (USA), NSERC (Canada), IHEP (China), CEA and CNRS-IN2P3 (France), BMBF and DFG (Germany), INFN (Italy), NFR (Norway), MIST (Russia), and PPARC (United Kingdom). Individuals have received support from the A. P. Sloan Foundation, Research Corporation, and Alexander von Humboldt Foundation.

REFERENCES

1. N. Cabibbo, Phys. Rev. Lett. **10**, 531 (1963); M. Kobayashi and T. Maskawa, Prog. Th. Phys. **49**, 652 (1973).
2. *BABAR* Collaboration, B. Aubert *et al.*, SLAC-PUB-9293, hep-ex/0207042, to appear in Phys. Rev. Lett. **.**
   BABAR Collaboration, B. Aubert *et al.*, Phys. Rev. Lett. **87**, 091801 (2001).
3. BELLE Collaboration, K. Abe *et al.*, Phys. Rev. Lett. **87**, 091802 (2001).
4. *BABAR* Collaboration, B. Aubert *et al.*, Nucl. Instr. and Methods A **479**, 1 (2002).
5. *BABAR* Collaboration, B. Aubert *et al.*, SLAC-PUB-9060, hep-ex/0201020, to appear in Phys. Rev. D **.**
6. *BABAR* Collaboration, B. Aubert *et al.*, this conference, SLAC-PUB-9293, hep-ex/0207042 to appear in Phys. Rev. Lett. **.**
7. *BABAR* Collaboration, B. Aubert *et al.*, Phys. Rev. Lett. **87**, 241801 (2001).
8. Method as in Hocker et al, Eur.Phys.J.C21:225-259,2001 and http://ckmfitter.in2p3.fr/
9. A.I. Sanda and Z.Z. Xing, Phys. Rev. D **56**, 341 (1997).
10. *BABAR* Collaboration, B. Aubert *et al.*, this conference, SLAC-PUB-9299, hep-ex/10207072.
11. *BABAR* Collaboration, B. Aubert *et al.*, this conference, SLAC-PUB-9298, hep-ex/0207058.
12. *BABAR* Collaboration, B. Aubert *et al.*, Phys. Rev. Lett. **87**, 151801-1 (2001).
13. *BABAR* Collaboration, B. Aubert *et al.*, this conference, SLAC-PUB-9297, hep-ex/0207070.
14. *BABAR* Collaboration, B. Aubert *et al.*, this conference, SLAC-PUB-9317, hep-ex/0207055. to appear in Phys. Rev. Lett.
15. M. Gronau and D. London, Phys. Rev. Lett. **65**, 3381 (1990).
16. Y.Grossman and H.R. Quinn Phys. Rev.

D **58**, 017504 (1998).
17. *BABAR* Collaboration, B. Aubert *et al.*, this conference, SLAC-PUB-9304, hep-ex/0207065.
18. *BABAR* Collaboration, B. Aubert *et al.*, this conference, SLAC-PUB-9310, hep-ex/0207063.
19. The *BABAR* Physics Book, Editors P.F. Harrison and H.R. Quinn, SLAC-R-504 (1998).
20. R. Aleksan, I. Dunietz, B. Kayser and F. Le Diberder, Nuclear Physics **B361**, 141 (1991).
21. *BABAR* Collaboration, B. Aubert *et al.*, this conference, SLAC-PUB-9303, hep-ex/0207068.
22. M. Gronau and D. Wyler, Phys. Lett. **B265**, 172 (1991); M. Gronau and D. London, Phys. Lett. **B253** 483 (1991).
23. D. Atwood, I. Dunietz and A. Soni, Phys. Rev. Lett. **78**, 3257 (1997).
24. *BABAR* Collaboration,B. Aubert *et al.* this conference, SLAC-PUB-9311, hep-ex/0207087.